Laser-enhanced high-intensity focused ultrasound heating in an in vivo small animal model

Janggun Jo, and Xinmai Yang

Articles you may be interested in

Laser-enhanced cavitation during high intensity focused ultrasound: An in vivo study
Applied Physics Letters **102**, 133702 (2013); 10.1063/1.4800780

Enhanced-heating effect during photoacoustic imaging-guided high-intensity focused ultrasound
Applied Physics Letters **99**, 231113 (2011); 10.1063/1.3669441

Laser-generated focused ultrasound for arbitrary waveforms
Applied Physics Letters **109**, 174102 (2016); 10.1063/1.4964852

Photoacoustic eigen-spectrum from light-absorbing microspheres and its application in noncontact elasticity evaluation
Applied Physics Letters **110**, 054101 (2017); 10.1063/1.4975373

Wavelet-transform-based active imaging of cavitation bubbles in tissues induced by high intensity focused ultrasound
The Journal of the Acoustical Society of America **140**, 798 (2016); 10.1121/1.4960519

Laser enhanced high-intensity focused ultrasound thrombolysis: An in vitro study
The Journal of the Acoustical Society of America **133**, EL123 (2013); 10.1121/1.4778375
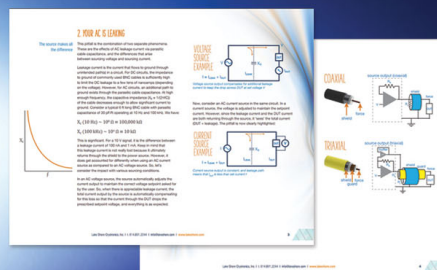
Laser-enhanced high-intensity focused ultrasound heating in an *in vivo* small animal model

Janggun Jo and Xinmai Yang[a)]

KU Bioengineering Research Center and Department of Mechanical Engineering, University of Kansas,
1530 W. 15th Street, 5109 Learned Hall, Lawrence, Kansas 66045, USA

The enhanced heating effect during the combination of high-intensity focused ultrasound (HIFU) and low-optical-fluence laser illumination was investigated by using an *in vivo* murine animal model. The thighs of murine animals were synergistically irradiated by HIFU and pulsed nanosecond laser light. The temperature increases in the target region were measured by a thermocouple under different HIFU pressures, which were 6.2, 7.9, and 9.8 MPa, in combination with 20 mJ/cm^2 laser exposures at 532 nm wavelength. In comparison with conventional laser therapies, the laser fluence used here is at least one order of magnitude lower. The results showed that laser illumination could enhance temperature during HIFU applications. Additionally, cavitation activity was enhanced when laser and HIFU irradiation were concurrently used. Further, a theoretical simulation showed that the inertial cavitation threshold was indeed decreased when laser and HIFU irradiation were utilized concurrently. *Published by AIP Publishing.* [http://dx.doi.org/10.1063/1.4968509]

High-intensity focused ultrasound (HIFU) is a non-invasive procedure that works through rapidly depositing high intensity acoustic energy into a small region to induce cell necrosis primarily by hyperthermia.[1,2] Besides thermal effects, mechanical effects such as acoustic cavitation also arise during a HIFU treatment.[3] Acoustic cavitation during the HIFU treatment is caused by the creation or motion of a vapor cavity due to a large negative pressure in the tissue or an elevated tissue temperature (boiling cavitation).[4] The rapid expansion and collapse of a cavitation bubble can generate high instantaneous pressures that will cause physical damage and enhance HIFU heating effects.[5–10]

Previously, we reported that the concurrent use of diagnostic laser and HIFU radiation could result in an enhanced cavitation activity.[11,12] The important feature was that the laser fluence needed to enhance cavitation was less than 50 mJ/cm^2 when laser and HIFU radiation were combined, which was lower by at least one order of magnitude than the optical fluence needed for optical breakdown or vaporization.[13,14] In the current study, we further investigated the enhanced heating effect when a diagnostic laser system was used concurrently with HIFU in an *in vivo* animal model. Laser light, whose fluence was limited by the safety standard recommended by American National Standards Institute (ANSI),[15] was used to illuminate the thighs of murine animals during the HIFU treatment. The enhanced cavitation activity and temperature rise were monitored by a passive cavitation detector (PCD) and a thermocouple, respectively. In addition, a potential mechanism based on photoacoustic (PA) cavitation was proposed to explain the enhanced cavitation activity during the concurrent use of low-optical-fluence laser and HIFU radiation.

A detailed schematic of the system[16–18] is shown in Figure 1. A tunable optical parameter oscillator (OPO) laser

(Surelite OPO PLUS, Continuum, Santa Clara, CA) pumped by a Q-switched, Nd:YAG laser with a pulse repetition rate of 10 Hz (~3 ns pulse width) was used as the light source. The laser light was directed by two prisms and a conical lens to form a ring-shaped illumination pattern. The laser beam was then focused by a condenser lens to make the laser beam confocal with a 5 MHz transducer (SU-108-013, Sonic Concepts, Bothell, WA). The 5 MHz transducer (35 mm focal length, 33 mm aperture size, and focal zone size: 0.32 mm × 2.95 mm) was located in the center of the condenser lens. A 10 MHz focused ultrasound transducer (V315, Olympus NDT, MA) that had a 37.5 mm focal length was used as a PCD. The PCD was positioned to be confocal with the HIFU transducer and the laser beam.

In this study, we used rats (Sprague Dawley, 200–250 g, male or female) for all of the *in vivo* experiments. All animals were handled and cared for in accordance with the Guide for the Care and Use of Laboratory Animals, and the procedures were approved by the Institutional Animal Care and Use Committee at the University of Kansas. During an experiment, an animal was initially anesthetized with a mixture of ketamine (87 mg/kg body weight) and xylazine (13 mg/kg body weight). The subsequent anesthesia was maintained with the inhalation of 1.0%–2.0% isoflurane mixed in pure oxygen. After the hair was removed from the region of interest, the anesthetized animal was fixed on a custom-designed animal holder, and the body temperature was maintained with a water circulating pad. A T-type thermocouple was inserted into the animal's leg through a fine needle. The tip of the thermocouple was located 0.5 mm away from the HIFU focal point. The animal was then coated with ultrasound gel and placed under an acoustic coupling membrane at the bottom of a water tank that was filled with degassed water. The heartbeat and blood oxygenation of the animal were monitored with a pulse-oximeter.

During each HIFU treatment, the source signal was generated by a function generator (HP33250A, Agilent

a)Author to whom correspondence should be addressed. Electronic mail: xmyang@ku.edu
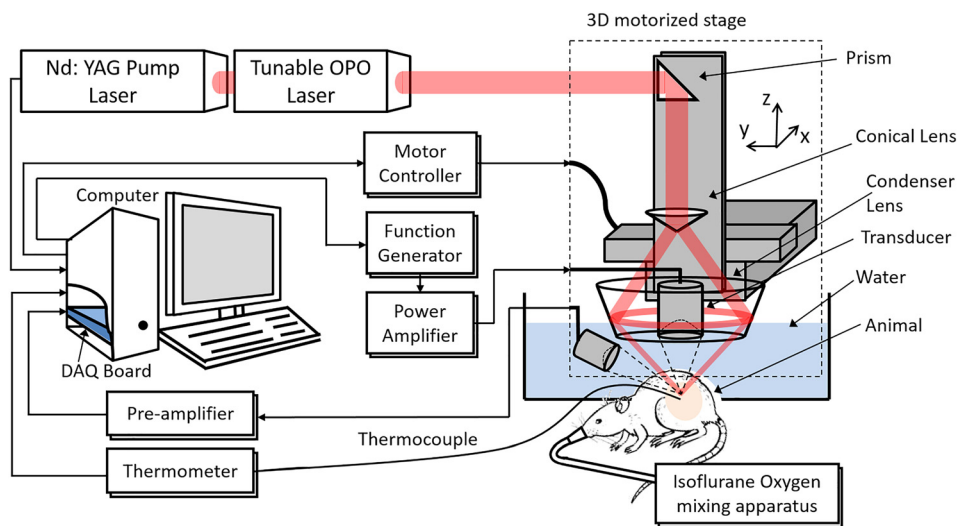
FIG. 1. The detailed schematic of the combined laser and HIFU therapeutic system.

Technologies, Santa Clara, CA) and amplified by a 50 dB radio frequency (RF) amplifier (350 L, ENI Technology Inc., Rochester, NY) before being delivered to the HIFU transducer. The laser pulses were delivered to the same region during the HIFU treatment. Cavitation signals detected by the PCD were amplified by a pre-amplifier (5072PR, Olympus NDT, Waltham, MA) and collected by a data acquisition card (GageScope, CS21G8256MSn Gage, Lockport, IL). A 10 MHz high-pass filter was used to remove contributions from the HIFU fundamental and second harmonic frequencies. The temperature increase was measured by the thermocouple through a measurement system (Omega, OMB-DAQ-2416, Stamford, CT) that collected data at a 10 Hz rate.

The experiment was conducted under three HIFU focal pressures (6.2 MPa, 7.9 MPa, and 9.8 MPa). At each HIFU pressure, we used 5 rats to collect five data points for averaging. On each rat, HIFU with laser irradiation was tested on one hind leg, and HIFU without laser irradiation was tested on the other hind leg. The corresponding HIFU focal pressures were obtained from a finite difference time domain (FDTD) algorithm[19] using acoustical properties of soft tissue (1540 m/s and 0.3 Np/cm at 5 MHz). The wavelength of the laser light was 532 nm.

Figure 2(a) shows an example of the measured temperatures with standard deviation (STD) from five HIFU sonications with and without laser illumination. With laser illumination, the temperature rise induced by HIFU was much higher, with a maximum of ∼14 °C difference between HIFU with laser and without laser. The corresponding cavitation signals received by the PCD are shown in Figures 2(b) and 2(c). Cavitation emissions were clearly enhanced while implementing HIFU with concurrent laser illumination.

To compare the temperature enhancement between different HIFU pressures, a temperature enhancement rate (TER) is defined as $R = T_{pkw}/T_{pkwo}$, where T_{pkw} is the peak temperature (in °C) with laser illumination, and T_{pkwo} is the peak temperature (in °C) without laser illumination. TERs for different HIFU pressures are shown in Figure 3. The largest TER, ∼1.4, was at 6.2 MPa, while the TER at 9.8 MPa was approximately 1, indicating no enhancement. This result may be due to the shielding effect of cavitation in the pre-focal region when HIFU pressure becomes large, which prevented acoustic waves from propagating to the focal region.[6] As a result, the addition of laser light might not enhance the temperature rise at the focal region at 9.8 MPa, where temperature was measured.

Laser irradiation has been widely used to initiate cavitation in clear media with high optical fluence.[13,14] In this study, however, we showed that, with the combination of laser and ultrasound, cavitation was enhanced at a very low optical fluence. The applied optical fluence complies with laser safety limits for human skin exposure recommended by ANSI.[15] At this optical fluence, optical breakdown and vaporization are unlikely. The temperature increase induced by the short-pulsed laser with a 3-ns pulse duration can be
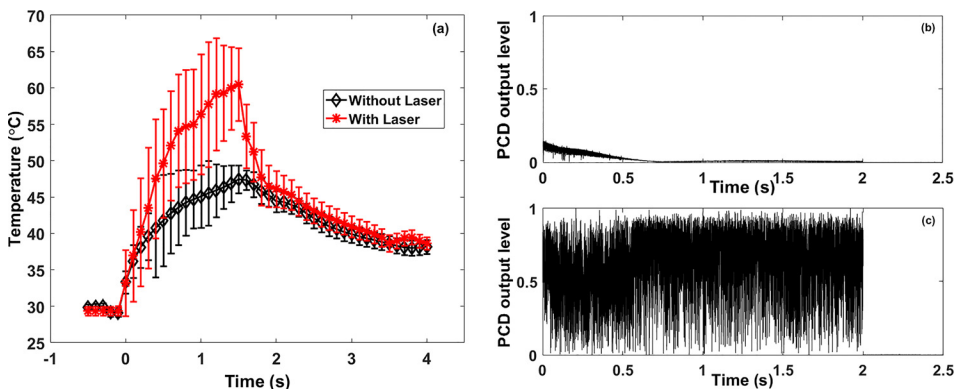

FIG. 2. (a) *In vivo* measured temperature resulting from HIFU with and without laser exposure. (b) An example of cavitation signals detected by the PCD with HIFU only. (c) An example of cavitation signals detected by the PCD with HIFU and laser exposure. HIFU was applied at a pressure of 6.2 MPa in the focal region that was 9 mm deep (through a layer of chicken breast), and the sonication duration was 2 seconds. For laser exposure, 532 nm wavelength light with 20 mJ/cm² surface fluence was used, which would produce about 2 mJ/cm² at the focal region.
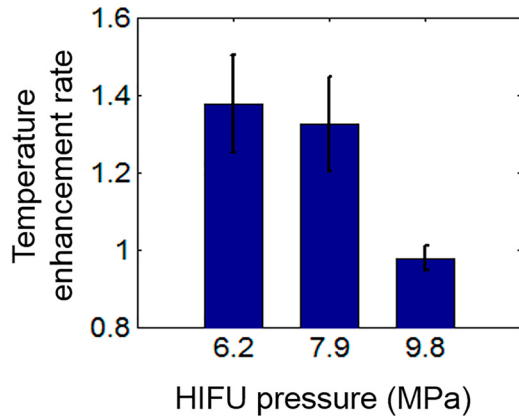
FIG. 3. Temperature enhancement rates at three HIFU focal pressures.

simply estimated by using the Pennes bioheat transfer equation (BHTE).[20] Because the heating process occurs on the time scale of nanoseconds, which is much faster than thermal diffusion, the thermal confinement condition applies.[21] Then the temperature rise can be estimated by $\rho C_p \Delta T = W$, where ΔT is the temperature rise, ρ is the density of the medium, C_p is the specific heat of the medium, $W = \mu_a F$ is the energy deposition per unit volume due to the absorption of laser energy, μ_a is the optical absorption, and F is the optical fluence. Under thermal confinement, the induced temperature is only $\sim 1\,^{\circ}$C when using $F = 20\,$mJ/cm^2 at 532-nm light. Here, $\rho = 1000\,$kg/m^3, C $= 4187\,$J/(kg K), and optical absorption $\mu_a = 244$/cm were used. This result is consistent with the conclusion in PA imaging studies, where similar levels of light intensity have been used. Since the induced temperature rise by laser pulses alone is small, its effect on cavitation is negligible. Therefore, the enhanced cavitation and heating effect showed in this study is due to the combined effect of laser and ultrasound irradiation, not laser irradiation alone.

The enhanced cavitation effect may be explained by examining the PA cavitation effect. Traditionally, PA cavitation refers to cavitation produced directly by PA waves without adding nanoparticles.[22–24] In recent years, another type of PA cavitation has been referenced in the literature, which is the generation of laser-induced vapor bubbles around plasmonic nanoparticles followed by applying an external ultrasound field.[25–29] The mechanisms of these two types of PA cavitation are very different. The former depends on strong PA waves generated through the PA effect (usually a converging PA wave), and the laser-induced temperature is much lower than the boiling temperature (therefore, termed cold cavitation). The latter relies on the photothermal effect to produce vapor bubbles (hot cavitation) on the surfaces of plasmonic nanoparticles. The current study is likely based on the traditionally defined PA cavitation, where cavitation may be produced directly by PA waves, with the assistance of ultrasound pulses and without using exogenous agents.

Paltauf et al.[22] have experimentally shown that cavitation can be induced when PA waves converge at the center of a spherical optical absorber. Their numerical results also demonstrated that, when the produced PA wave by a spherical optical absorber converged at the center of the absorber, a strong, nearly negative-only acoustic pulse was produced. The rarefaction pressure of the acoustic pulse strongly

depends on the size and optical absorption of the target as well as the pulse width of the laser beam. The resulting peak rarefaction pressure can easily exceed 10 MPa. One estimate made by Sun and Gerstman[30] showed that the peak rarefaction pressure could be as high as 1000 MPa in melanosome, an extremely strong optical absorber in soft tissue. Given these huge rarefaction pressures, cavitation is likely in blood vessels and melanoma cells.

To understand how laser-produced PA waves affect cavitation when combined with HIFU, we employed a bubble dynamic model to investigate the behavior of a bubble when a synchronized external ultrasound field is applied with a laser pulse. The generation and propagation of PA waves can be modeled by the following wave equation:[21]

$$\nabla^2 p - \frac{1}{c}\frac{\partial^2 p}{\partial t^2} = -\frac{\beta}{C_p}\frac{\partial H}{\partial t},\tag{1}$$

where p is the acoustic pressure, c is the sound speed in the medium, β is the thermal expansion coefficient, C_p is the specific heat capacity at constant pressure, and H is the heating function.

Given that stress confinement and thermal confinement are satisfied during PA wave generation, the initial pressure distribution can be expressed by[21] $p_0(r) = \mu_a \Gamma F(r)$, where μ_a is the optical absorption coefficient, Γ is the Gruneisen constant, and $F(r)$ is the local optical fluence. At body temperature (37 $^{\circ}$C), the Gruneisen parameter Γ is around 0.20 for blood. The absorption coefficient of blood at 532 nm of wavelength is assumed to be 244 cm^{-1}. If the laser light had a fluence of 20 mJ/cm^2, as we used in the experiments, the calculated initial PA pressure would be 0.98 MPa at the surface.

Based on the wave propagation equation,[23,24,30] when a cylindrically shaped blood vessel is illuminated by a laser pulse, significant rarefaction pressures can be produced at its center region through PA wave propagation. Figure 4(a) shows the simulated PA wave observed near the center (r = 1 μm) of a 200-μm diameter blood vessel when it was illuminated by a 3-ns laser pulse.

To study the subsequent bubble dynamics, the Keller–Miksis equation is used, which has the following form:[31,32]

$$\left(1 - \frac{\dot{R}}{c}\right)R\ddot{R} + \frac{3}{2}\left(1 - \frac{\dot{R}}{3c}\right)\dot{R}^2$$
$$= \frac{R}{\rho c}\frac{d}{dt}[p_B] + \frac{1}{\rho}\left(1 + \frac{\dot{R}}{c}\right)\left(p_B - p_\infty - p\left(t + \frac{R}{c}\right)\right),\tag{2}$$

where dots denote time derivatives, R is the bubble radius, t is the time, c is the speed in the surrounding medium, ρ is the density of the surrounding medium, p_∞ is the pressure at infinity, and p_B is the pressure at the surrounding medium side of the interface between the medium and the bubble. p_B is given by the following formula: $p_B = p_g - \frac{2\sigma}{R} - \frac{4\mu}{R}\dot{R}$, where p_g is the pressure inside the bubble, σ is the surface tension coefficient, and μ is the viscosity of the fluid.

With the Keller–Miksis equation, we calculated the change in bubble radius when a cavitation nucleus with a
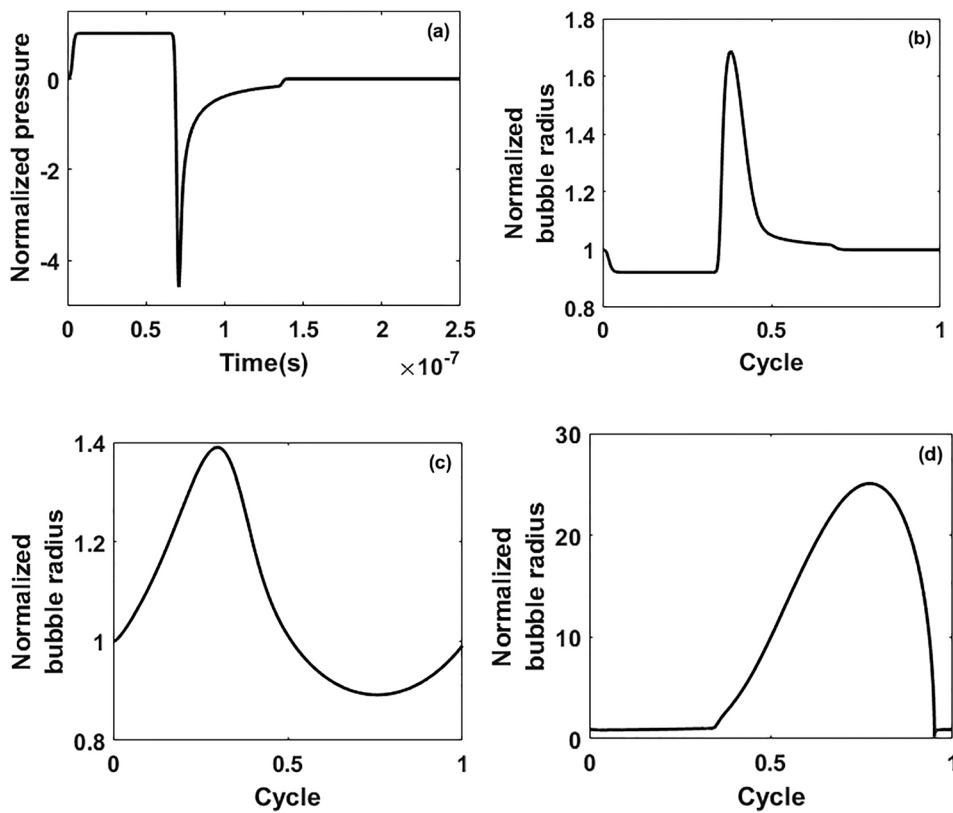
FIG. 4. (a) PA signal produced near the center of a 200-μm blood vessel due to wave propagation. (b) The radius of a 50-nm bubble when it was driven by the PA pulse in (a). (c) The radius of a 50-nm bubble when it was driven by an ultrasound pulse. (d) The radius of a 50-nm bubble when it was driven by synchronized ultrasound and laser pulses, where the laser pulse was applied 38 ns before the ultrasound pulse at the target. The blood vessel was illuminated with an optical fluence of 20 mJ/cm^2. The optical absorption was assumed to be 244/cm. The ultrasound driven frequency was 5 MHz and the driven pressure was 1.5 MPa. Bubble radius was normalized by the equilibrium radius, which is 50 nm. The pressure was normalized by p_0.

size of 50 nm was present in the PA wave field. Figure 4(b) shows that the spike-like radial motion was produced, which essentially followed the shape of the original PA wave. If a 5-MHz ultrasound pulse with an amplitude of 1.5 MPa was utilized to drive the same cavitation nucleus, the change in bubble radius was around 40%, as shown in Figure 4(c). However, when the PA pulse and the ultrasound pulse are synergistically applied together, as shown in Figure 4(d), the oscillation of the bubble exhibited strong non-linearity, with a maximum radius of nearly 27 times of the equilibrium radius.

Fig. 5 shows the maximum bubble radius when the laser pulse was applied at a specified delay time. For a 5 MHz ultrasound signal, the maximum bubble radius occurs when the delay time is −38 ns (Fig. 5(a)), while for a 1 MHz ultrasound signal, the maximum bubble radius occurs when the delay time is 91 ns (Fig. 5(b)). Here, we assumed that the beginning of the ultrasound pulse was 0 ns. For the 5 MHz ultrasound signal with the laser pulse at −38 ns delay time, the negative peak of the PA wave superposes on the ultrasound pulse at 32 ns, which corresponds to a phase of

58 degrees. For the 1 MHz ultrasound signal with the laser pulse at 91 ns delay time, the negative peak of the PA wave superposes on the ultrasound pulse at 161 ns, which also corresponds to a phase of 58 degrees. These optimal delay times were used for the following calculations.

Figure 6(a) shows the inertial cavitation (IC) threshold (i.e., the peak negative pressure threshold) calculated under different laser fluences at 5 MHz for a 200 μm blood vessel. It shows that the synergistically applied laser pulses can significantly reduce the threshold pressure for IC, indicating that the likelihood of IC will greatly increase. The impact on the IC threshold reduces as the laser fluence decreases. We have previously measured an IC threshold of 9.5 MPa at 5 MHz with HIFU alone.[33] This would correspond to a bubble equilibrium radius of about 8 nm in the simulation. Based on the simulation, with a laser fluence of 2 mJ/cm^2 at 532 nm, the IC threshold will reduce from 9.5 MPa to 9.2 MPa for an 8 nm bubble. However, we currently observed IC at 7.9 MPa (for 4 out of 5 animals), which is lower than the theoretical prediction. This discrepancy could be due to the presence of the thermocouple (metal) near the
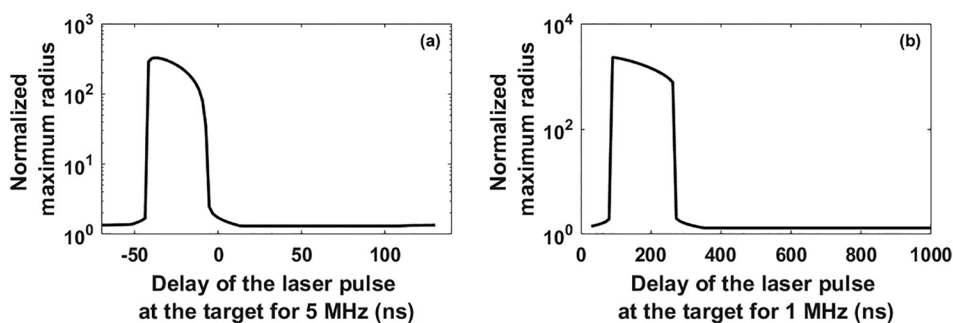

FIG. 5. The maximum bubble radius when a laser pulse was applied to a 10-nm bubble at a specified delay time after a (a) 5-MHz ultrasound pulse and (b) a 1 MHz ultrasound pulse of 6.5 MPa. The maximum bubble radius is normalized by 10 nm.
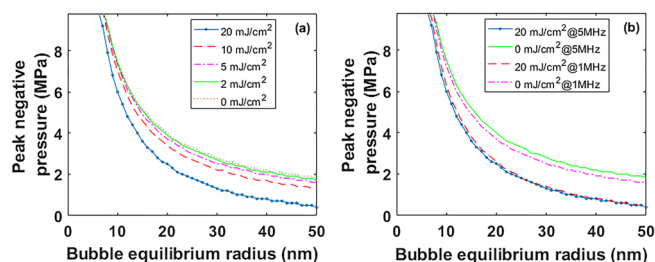
FIG. 6. (a) Calculated IC threshold for 5 MHz ultrasound signal with different laser fluences. (b) Calculated IC threshold for 1 MHz and 5 MHz ultrasound signals. Inertial cavitation occurs when $R_{max}/R_0 > 2$, where R_{max} is the maximum radius of an oscillating bubble and R_0 is the equilibrium radius of the bubble. A 3-ns laser pulse is assumed. The optical absorption is assumed to be 244/cm.

focal zone, which may also reduce the IC threshold.[34] Additionally, more accurate information about the size distribution of cavitation nuclei and blood vessel diameters will be needed for a more precise theory, which should be pursued in future.

Figure 6(b) shows the IC thresholds for 1 and 5 MHz ultrasound signals. All thresholds were calculated with the optimal delay times at the corresponding frequencies. It is interesting to note that when there is no laser, the IC threshold at 5 MHz is higher than at 1 MHz; with laser, the IC threshold at 1 MHz is slightly higher than at 5 MH. This indicates that, with the current parameters (laser pulse length and blood vessel size), PA waves have a greater impact on the IC threshold at 5 MHz than at 1 MHz. This may suggest that optimal ultrasound frequency exists for a given PA wave, which may be worth further investigation.

In conclusion, we have demonstrated that the combination of low-optical-fluence laser light and HIFU could enhance HIFU heating *in vivo* by reducing IC threshold. PA cavitation may play a significant role in this application. A limitation of this technique is the treatment depth. Our current and previous results demonstrated a maximum treatment depth of around 1 cm. Deeper treatment depth will require higher laser fluence at skin surface, or special methods to deliver laser light, such as using an optical fiber to deliver laser energy to the target region. Additionally, the size distribution of blood vessels and cavitation nuclei will have significant impact on the result and should be studied in future work.

[1]J. E. Kennedy, Nat. Rev. Cancer **5**(4), 321–327 (2005).
[2]J. E. Kennedy, F. Wu, G. R. ter Haar, F. V. Gleeson, R. R. Phillips, M. R. Middleton, and D. Cranston, Ultrasonics **42**(1–9), 931–935 (2004).
[3]T. J. Dubinsky, C. Cuevas, M. K. Dighe, O. Kolokythas, and J. H. Hwang, AJR, Am. J. Roentgenol. **190**(1), 191–199 (2008).
[4]V. A. Khokhlova, M. R. Bailey, J. A. Reed, B. W. Cunitz, P. J. Kaczkowski, and L. A. Crum, J. Acoust. Soc. Am. **119**(3), 1834–1848 (2006).
[5]X. Yang, R. A. Roy, and R. G. Holt, J. Acoust. Soc. Am. **116**(6), 3423–3431 (2004).
[6]R. G. Holt and R. A. Roy, Ultrasound Med. Biol. **27**(10), 1399–1412 (2001).
[7]C. C. Coussios, C. H. Farny, G. T. Haar, and R. A. Roy, Int. J. Hyperthermia **23**(2), 105–120 (2007).
[8]X. M. Yang and C. C. Church, Acoust. Res. Lett. Online-Arlo **6**(3), 151–156 (2005).
[9]S. J. Guo, Y. Jing, and X. N. Jiang, IEEE Trans. Ultrason. Ferroelectr. Freq. Control **60**(8), 1699–1707 (2013).
[10]B. C. Tran, J. Seo, T. L. Hall, J. B. Fowlkes, and C. A. Cain, IEEE Trans. Ultrason. Ferroelectr. Freq. Control **50**(10), 1296–1304 (2003).
[11]H. Z. Cui and X. M. Yang, Appl. Phys. Lett. **99**(23), 231113 (2011).
[12]H. Cui and X. Yang, J. Acoust. Soc. Am. **133**(2), EL123–EL128 (2013).
[13]A. Vogel, J. Noack, K. Nahen, D. Theisen, S. Busch, U. Parlitz, D. X. Hammer, G. D. Noojin, B. A. Rockwell, and R. Birngruber, Appl. Phys. B Lasers Opt. **68**(2), 271–280 (1999).
[14]W. Lauterborn, Acustica **31**(2), 51–78 (1974).
[15]*American National Standard for Safe Use of Lasers ANSI Z136.1-2007*, Section 8 (Laser Institute of America, Orlando, FL, 2007).
[16]H. Cui, J. Staley, and X. Yang, J. Biomed. Opt. **15**, 021312 (2010).
[17]H. Cui and X. Yang, Med. Phys. **38**(10), 5345–5350 (2011).
[18]H. Z. Cui and X. M. Yang, Med. Phys. **37**(9), 4777–4781 (2010).
[19]I. M. Hallaj and R. O. Cleveland, J. Acoust. Soc. Am. **105**(5), L7–L12 (1999).
[20]H. H. Pennes, J. Appl. Physiol. **1**(2), 93–122 (1948).
[21]L. V. Wang and H.-I. Wu, *Biomedical Optics: Principles and Imaging* (John Wiley & Sons, Inc., Hoboken, New Jersey, 2007).
[22]G. Paltauf and H. Schmidt-Kloiber, Appl. Phys. A Mater. Sci. Process. **68**(5), 525–531 (1999).
[23]G. Paltauf and P. E. Dyer, Chem. Rev. **103**(2), 487–518 (2003).
[24]J. M. Sun, B. S. Gerstman, and B. Li, J. Appl. Phys. **88**(5), 2352–2362 (2000).
[25]B. Arnal, C. W. Wei, C. Perez, T. M. Nguyen, M. Lombardo, I. Pelivanov, L. D. Pozzo, and M. O'Donnell, Photoacoustics **3**(1), 11–19 (2015).
[26]B. Arnal, C. Perez, C. W. Wei, J. J. Xia, M. Lombardo, I. Pelivanov, T. J. Matula, L. D. Pozzo, and M. O'Donnell, Photoacoustics **3**(1), 3–10 (2015).
[27]C. H. Farny, T. M. Wu, R. G. Holt, T. W. Murray, and R. A. Roy, Acoust. Res. Lett. Online-Arlo **6**(3), 138–143 (2005).
[28]J. R. McLaughlan, R. A. Roy, H. Ju, and T. W. Murray, Opt. Lett. **35**(13), 2127–2129 (2010).
[29]H. Ju, R. A. Roy, and T. W. Murray, Biomed. Opt. Express **4**(1), 66–76 (2013).
[30]J. M. Sun and B. S. Gerstman, Phys. Rev. E **59**(5), 5772–5789 (1999).
[31]X. M. Yang and C. C. Church, J. Acoust. Soc. Am. **118**(6), 3595–3606 (2005).
[32]C. C. Coussios and R. A. Roy, Annu. Rev. Fluid Mech. **40**, 395–420 (2008).
[33]H. Cui, T. Zhang, and X. Yang, Appl. Phys. Lett. **102**(13), 133702 (2013).
[34]C. P. Labuda and C. C. Church, Ultrasound Med. Biol. **37**(3), 442–449 (2011).